Preparation, Characterization, and Properties of Environmentally Friendly Waterborne Poly(urethane acrylate)/Silica Hybrids

Dongmei Wu, Fengxian Qiu, Heping Xu, Jingli Zhang, Dongya Yang

School of Chemistry and Chemical Engineering, Jiangsu University, Zhenjiang 212013, China

Received 5 January 2010; accepted 23 May 2010
DOI 10.1002/app.32846
Published online 19 August 2010 in Wiley Online Library (wileyonlinelibrary.com).

ABSTRACT: A series of environmentally friendly waterborne poly(urethane acrylate) (WPUA)/silica (SiO_2) hybrids were synthesized by a sol–gel process on the basis of isophorone diisocyanate, polyester polyol (GE-210), dimethylpropionic acid, butyl acrylate and methyl methacrylate monomers, tetraethoxysilane (TEOS), and 3-glycidyloxypropyl trimethoxysilane (GLYMO) as a coupling agent. The mechanical properties of the WPUA/SiO_2 hybrids were investigated through tensile and hardness tests. Fourier transform infrared spectroscopy, scanning electron microscopy, transmission electron microscopy, atomic force microscopy, and X-ray diffraction were used to assess the fracture surface morphology and the dispersions of the WPUA/SiO_2 hybrids. The strength and hardness values of the WPUA/SiO_2 hybrids were improved significantly. This was attributed to the synergistic effect of WPUA, GLYMO, and TEOS. The results show that SiO_2 particles of the membranes had a uniform dispersion and formed an excellent interfacial bonding layer on their surfaces. The prepared hybrids showed good thermal stability and mechanical properties in comparison with pure WPUA and showed tunable transparence with the SiO_2 fraction in the film. Through suitable adjustment of the TEOS content, some thin hybrids have potential applications as specialty materials. J Appl Polym Sci 119: 1683–1695, 2011

Key words: mechanical properties; polyurethanes; TEM; transparency

INTRODUCTION

Polyurethane (PU) materials are known to offer high performance with their toughness, mechanical flexibility, chemical resistance, and strong adhesion. Waterborne polyurethane (WPU) has become a major research and development fields in recent years because of its environmental friendliness, good processability, and good mechanical properties.[1,2] However, WPU has some drawbacks, such as weak water resistance, low adhesion in moist environments, relatively low heat resistance, and low mechanical properties; these inhibit the extensive application of WPU in coatings and adhesives. To compensate for these drawbacks, many researchers have modified WPU by crosslinking reactions and hybridization with epoxy, acrylate, and organosilicon.[3–5] Compared with the PU resin, polyacrylate (PA)-type products show outstanding performance in weatherability, water resistance, and solvent resistance; therefore, there are complementary roles in the performances of PU and PA. According to these characteristics, some methods have been used for the modification of WPU with acrylic resin.[6–8] The modified WPU emulsions had the advantages of both PU and PA; therefore, it is known as a third-generation WPU.[9–11]

In recent years, hybrid particles consisting of an inorganic core and a polymer shell, because of the possibility of combining the advantages of different materials, have attracted much attention from material scientists and researchers. For instance, composite particles have been designed to enhance the overall performance of composites in their mechanical and photonics properties.[12–14] The synergistic combination of organic polymer–inorganic hybrids is obtained via a sol–gel process. Since the 1970s, the sol–gel process has been used for the deposition of inorganic minerals *in situ* in an organic polymer matrix. The starting materials for the sol–gel process are metal alkoxides [$M(OR)_n$'s] and a small amount of acid or base as a catalyst. The metal alkoxides are hydrolyzed, and metal hydroxides

Correspondence to: F. Qiu (fxqiuchem@163.com).
Contract grant sponsor: Natural Science of Jiangsu Province; contract grant number: BK2008247.
Contract grant sponsor: China Postdoctoral Science Foundation; contract grant number: 20070420973.
Contract grant sponsor: Jiangsu Planned Projects for Postdoctoral Research Funds; contract grant number: 0602037B.

[$M(OH)_n$'s] are formed. The reaction is shown as follows:

$$M(OR)_n + nH_2O \rightarrow M(OH)_n + nROH$$

where M is Na, Ba, Cu, Al, Si, Ti, Ge, V, W, and so on; R is —CH_3, —C_2H_5, —C_3H_7, —C_4H_9, and so on; and $M(OH)_n$ is a reactive, three-dimensional network containing —O—M—O—M— linkages formed by the polycondensation of $M(OH)_n$ with $M(OR)_n$ or $M(OH)_n$.[15] The sol–gel methodology provides an easy, cost-effective, and excellent way to incorporate inorganic compounds into an organic binder. Therefore, the sol–gel method has been widely used to produce homogeneous microstructures and coatings with organic–inorganic hybrid solids at a relatively low temperature.[16–18]

To improve the compatibility between the organic and inorganic phases, it is essential to establish chemical linkages between the soft organic phase and the hard inorganic phase. This can be achieved with coupling agents, such as amine-terminated alkoxysilanes (e.g., 3-aminopropyl triethoxysilane), epoxy-capped alkoxysilanes [e.g., 3-glycidyloxypropyl trimethoxysilane (GLYMO)], isocyanato-capped alkoxysilanes (e.g., 3-triethoxysilylpropyl isocyanate), and so on.[19,20]

Zhang et al.[6] reported the synthesis and properties of polydimethylsiloxane (PDMS)-modified PU–acrylic hybrid emulsions by a solvent-free method. The emulsion particle size was uniform and around 45 nm, which ensured better performance of the formed film. The obtained Si–poly(urethane acrylate) (PUA) proved to possess a higher contact angle and better water resistance when the PDMS content was higher than 6.5%. The mechanical properties changed greatly when the PDMS content was above 6.5%. Bonilla et al.[21] successfully prepared PU/poly(methyl methacrylate)/silica (SiO_2) hybrid materials using 3-(trimethoxysilyl)propyl methacrylate and isocyanatopropyl triethoxysilane as dual coupling agents and tetraethoxysilane (TEOS)*in situ* bulk polymerization to improve their optical transparency. Guo et al.[22] reported the preparation of SiC nanoparticles to be incorporated into the PU matrix using the surface-initiated polymerization method. Hu et al.[7] used the oil-solubility initiator azobisisobutyronitrile (AIBN) to prepare PU–acrylate hybrid emulsions and study the influence of the initiator AIBN on the synthesis and properties of PU–acrylate hybrid emulsions. Yeh et al.[15] successfully prepared primary-amino-terminated WPU–SiO_2 hybrid materials by a sol–gel process without the addition of an external catalyst.

In this study, we used the epoxy-capped alkoxysilane coupling agent GLYMO as the precursor, which provided two different reactive functionalities, namely, an organic functional epoxy group and the inorganic alkoxysilane $Si(OCH_3)_3$ group. It had the ability to simultaneously form an organic network through the reaction of the organic functional epoxy group with the organic PUA and also an inorganic SiO_2 network with TEOS through the hydrolysis and subsequent condensation reactions of alkoxy silane groups. A series of waterborne poly(urethane acrylate) (WPUA)/SiO_2 hybrids were prepared by the sol–gel technique. The synthesized hybrids were characterized with Fourier transform infrared (FTIR) spectroscopy, ultraviolet–visible (UV–vis) spectroscopy, scanning electron microscopy (SEM), transmission electron microscopy (TEM), X-ray diffraction (XRD), differential scanning calorimetry (DSC), and atomic force microscopy (AFM) methods. Other properties of the WPUA/SiO_2 hybrids, such as the tensile strength, hardness, and water resistance values, were also determined.

EXPERIMENTAL

Materials

Polyester polyol (GE-210; 56 mg of KOH/g) was produced by Yutian Petrochemical Co. (Qingdao, China). Isophorone diisocyanate (IPDI) was supplied by HUL Co. (Krefeld, Germany). Dimethylpropionic acid (DMPA) was produced by PERSTOP Co. (Helsingborg, Sweden). *N*-Methyl-2-pyrrolidone, acetone, dibutylbis
(lauroyloxy)tin, triethylamine, TEOS, butyl acrylate (BA), methyl methacrylate (MMA), and AIBN were obtained from Guoyao Chemical, Ltd. (Shanghai, China). GLYMO was purchased from Nanjing Shuguang Chemical Plant (Nanjing, China). Hydroxyethyl methyl acrylate was purchased from Yinlian Chemical, Ltd. (Wuxi, Jiangsu, China).

Preparation of the WPUA dispersion

Polymerization was performed in a 250-mL, round-bottom, four-necked separable flask with a mechanical stirrer, thermometer, and condenser with a drying tube. GE-210, IPDI, and dibutylbis(lauroyloxy)tin as a catalyst were charged into the dried flask. With stirring, the mixture was heated to 85°C for about 2 h to obtain the NCO-terminated prepolymer. A certain amount of DMPA dissolved in *N*-methyl-2-pyrrolidone was added the prepolymer at 80–85°C for another 2 h so that the NCO-terminated prepolymer containing carboxyl group was obtained. Then, the reactant was diluted by a small amount of acetone to decrease the viscosity. Then, the reactants were cooled to 60°C, and hydroxyethyl methyl acrylate was added dropwise for 5 h. The prepolymer with an ethylene linkage was obtained, and the neutralizing

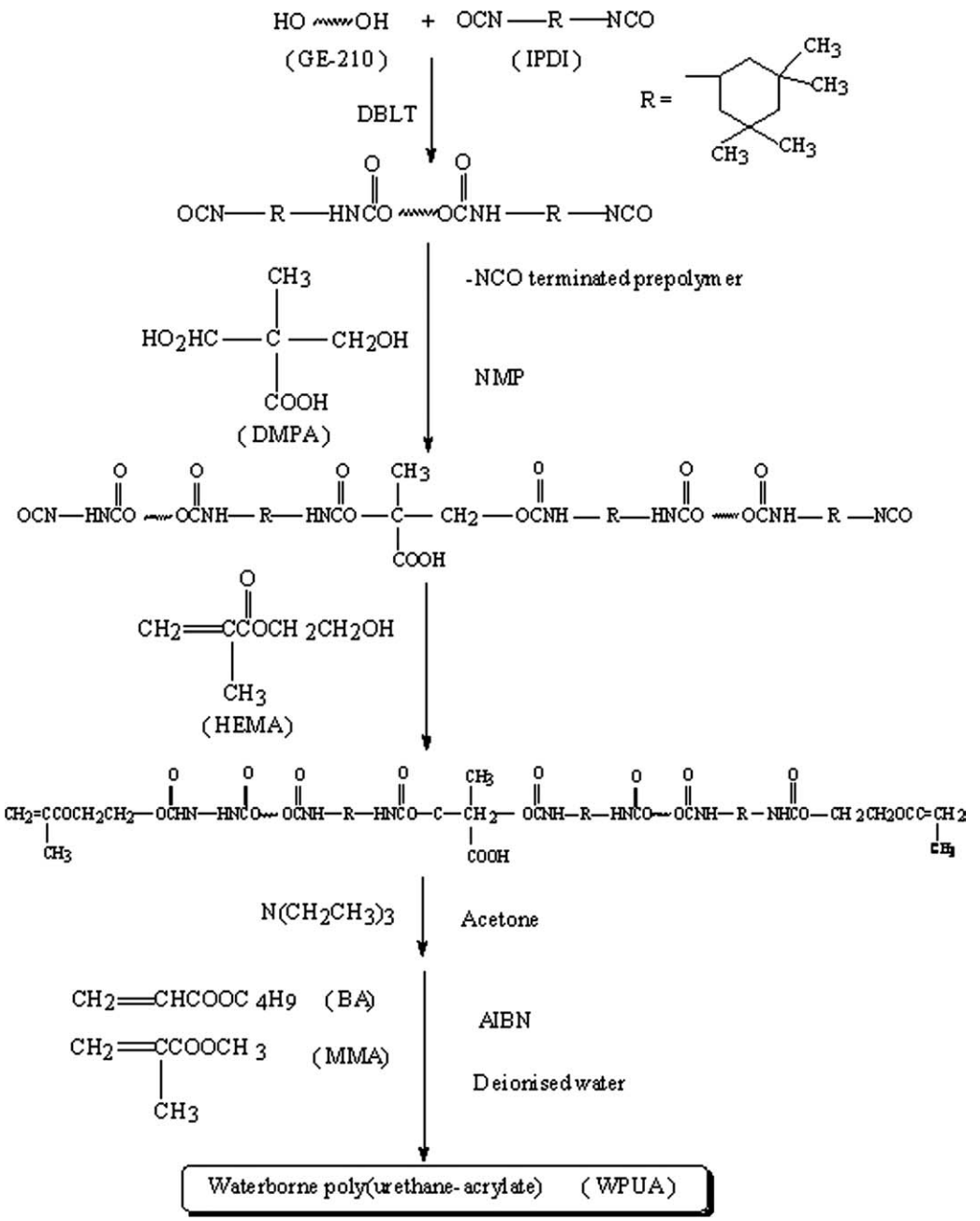

Scheme 1 Synthetic route of WPUA

solution, triethylamine, was added and stirred for 30 min with the temperature maintained at 40°C. The mixture of calculated BA and MMA was added to the prepolymer. The prepolymer/monomer mixture was then dispersed into deionizer water under vigorous stirring. AIBN was added to the dispersion subsequently. The WPUA aqueous dispersion was prepared after the copolymerization of vinyl monomers at 70°C. The synthetic route of the WPUA dispersion is shown in Scheme 1. The amounts of each chemical used for the synthesis are listed in Table I.

Preparation of the WPUA/SiO_2 hybrid material dispersion

WPUA/SiO_2 hybrid material dispersions containing different inorganic contents were synthesized via a sol–gel process.[16–18] In this study, a homogeneous organic solution was obtained from the coupling agent GLYMO and WPUA at 40°C for 1 h. The homogeneous inorganic solution was a hydrolyzed TEOS mixture, which was prepared with deionized water, hydrochloric acid, ethanol, and TEOS in a conical flask, and was stirred for 1 h. Then, it was added carefully to the organic solution and reacted

TABLE I
Reactant Summarizes of WPUA and Hybrids

Sample	GLYMO (g)	TEOS (wt %)	BA (g)	MMA (g)	GE-210 (g)	IPDI (g)
WPUA	0	0	9.625	4.125	10	10
Hyb-1	0.215	0.3	9.625	4.125	10	10
Hyb-2	0.333	0.5	9.625	4.125	10	10
Hyb-3	0.444	1.0	9.625	4.125	10	10
Hyb-4	0.666	1.5	9.625	4.125	10	10
Hyb-5	0.888	2.0	9.625	4.125	10	10
Hyb-6	1.333	3.0	9.625	4.125	10	10

for another 1 h. The temperature was cooled to room temperature and kept stirring for 12 h. The precursor, GLYMO, had two different reactive functionalities, namely, the organic functional group and the inorganic alkoxysilane group. GLYMO has the ability to simultaneously form an organic network through the reaction of the organic functional groups with the organic binder and also an inorganic SiO_2 network through the hydrolysis and subsequent condensation reactions of alkoxy silane groups. Therefore, with various proportions of GLYMO and TEOS, a series of WPUA/SiO_2 hybrids were obtained. In this article, the hybrids with different TEOS contents of 0.3, 0.5, 1.0, 1.5, 2.0, and 3.0% are expressed as Hyb-1, Hyb-2, Hyb-3, Hyb-4, Hyb-5, and Hyb-6, respectively, as shown in Table I. The synthetic route of the WPUA/SiO_2 hybrids is shown in Scheme 2.

In this experiment, when the TEOS content was greater than 3%, the hybrid dispersion was instable and appeared as a gel. Therefore, experiments with greater percentages of SiO_2 were not done.

Membrane preparation of the WPUA and WPUA/SiO_2

We prepared the membranes by casting the newly synthesized WPUA or hybrid dispersions onto polytetrafluoroethylene at room temperature for 2 days; this was followed by drying at 60°C for 3 h. This trend of drying was just for slow drying. It was also possible to evaporate the solvent at a fixed temperature, either room temperature or an elevated temperature. After demolding, the films were stored in a desiccator at room temperature for further studies.

Measurements and characterization

Apparent viscosity of the WPUA and WPUA/SiO_2 dispersions

The apparent viscosities of the WPUA and WPUA/SiO_2 dispersions were measured by a numerical viscometer (NDJ-9S, Shanghai Precision and Scientific Instrument Co., Ltd., Shanghai, China); when the shear rate was 2000 s^{-1}, the high shear rate warranted highly reliable measurements at a temperature 25°C

Particle size and particle size distribution (PSD) of the WPUA and WPUA/SiO_2 dispersions

The WPUA and WPUA/SiO_2 samples were added to 100-mL test tubes and diluted with deionized water. The particle diameter and PSD of the WPUA and WPUA/SiO_2 dispersions were measured by a laser particle size analyzer (BIC-9010, Brookhaven Instrument Co.) (Holtsville, New York, USA).

Surface tension (σ) of the WPUA and WPUA/SiO_2 dispersions

σ is an important parameter of the physical properties for the application performances of materials. In this study, the measurement of σ was conducted on a single-tube manner setup by the maximum air bubble method, as shown in Figure 1.

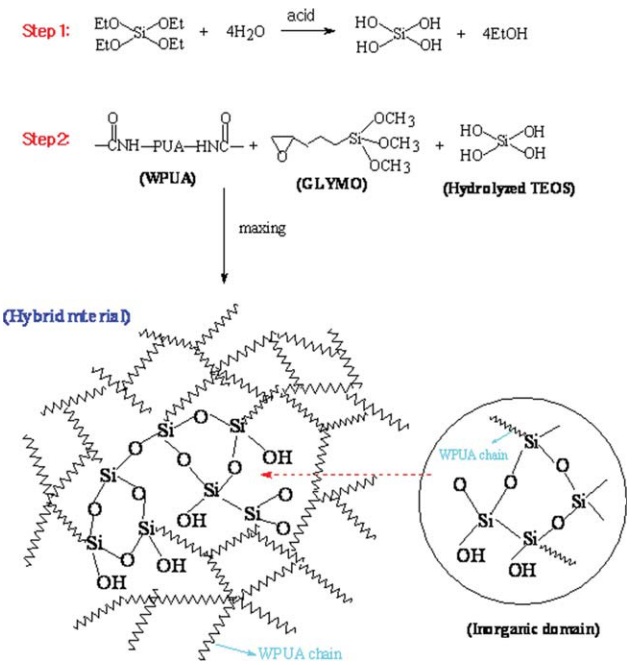

Scheme 2 Synthetic route of the WPUA/SiO_2 hybrid material dispersion. [Color figure can be viewed in the online issue, which is available at wileyonlinelibrary.com.]

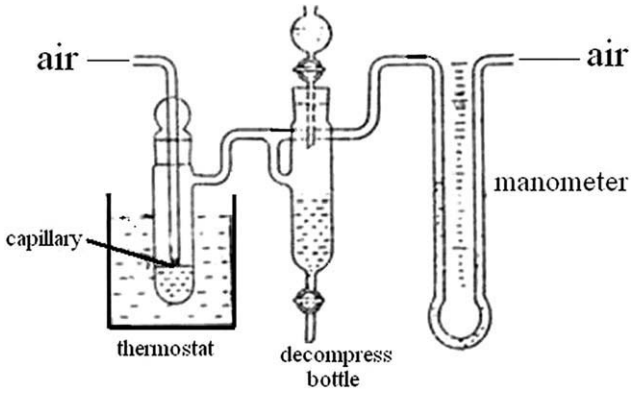

Figure 1 Measurement of σ.

When the liquid end of the capillary was tangent with the sample's liquid end, the liquid went up along the capillary. A piston of the tap funnel was opened, and water dropped slowly to reduce the system pressure. In this way, the liquid surface of the capillary had a bigger pressure than that of the cuvette, and a pressure difference was formed. When the pressure, which was the result of the pressure difference acting on the capillary surface, was a little larger than σ of the capillary nozzle liquid, the air bubble transgressed from the capillary nozzle. The maximum pressure was obtained from a manometer (DP-AW, Sangli Electronic Plant) (Nanjing, China), and the value is expressed by eq. (1):

$$P_{\max} = P_{\text{air}} - P_{\text{system}} = \Delta P \tag{1}$$

where $P_{\max}$ was the maximum pressure, P_{air} was atmospheric pressure, P_{system} was the pressure of system, and ΔP was differential value of P_{air} and P_{system}. When the air bubble transgressed from the capillary nozzle, the pressure was $\pi r^2 P_{\max}$, where r is the radius of the capillary. The pressure, which was brought by σ of the air bubble in the capillary, was $2\pi r\sigma$. The two pressure values were equal and are described by eq. (2):

$$\pi r^2 P_{\max} = \pi r^2 \Delta P = 2\pi r\sigma, \qquad \sigma = \left(\frac{r}{2}\right)\Delta P \tag{2}$$

When the same capillary was used, the σ values of different liquids were determined by eq. (3)

$$\frac{\sigma_1}{\sigma_2} = \frac{\Delta P_1}{\Delta P_2} \tag{3}$$

where P_1 was the maximum pressure of the measured liquid, and P_2 was the maximum pressure of the standard substance. σ of the different liquids could be obtained when the standard substance was measured (e.g., distilled water σ = 72 mN/m).

Tensile strength and elongation at break of the WPUA and WPUA/SiO_2 membranes

Tensile strength testing and elongation at break testing for all of the specimens were carried out on a tensile tester (KY-8000A, Jiangdu Kaiyuan Test Machine Co., Ltd., Jiangdu, China) at room temperature at a speed of 50 mm/min. All measurements had an average of three runs. The dumbbell-type specimen was 30 mm long at two ends, 0.2 mm thick, and 4 mm wide at the neck.

Hardness of the WPUA and WPUA/SiO_2 membranes

The hardness was measured with a sclerometer (KYLX-A, Jiangdu Kaiyuan Test Machine Co., Ltd., Jiangdu, China); measurements were done three times for each WPUA/SiO_2 sample, and the average value was calculated.

Water absorption of the WPUA and WPUA/SiO_2 membranes

Water absorption values of the WPUA or WPUA/SiO_2 membranes were obtained as follows: preweighed dry membranes (20 × 20 mm^2) were immersed in distilled water at 25°C. After 24 h, the membranes were then blotted with filter paper and weighed. The water absorption (w) was calculated as follows:

$$w = \frac{(m_2 - m_1)}{m_1} \times 100\% \tag{4}$$

where m_1 is the weight of the original dry sample and m_2 is the weight of the swollen sample.

Structure characterization and optical transparency

FTIR spectra of the WPUA and WPUA/SiO_2 membranes were obtained between 4000 and 400 cm^{-1} on a KBr powder with an FTIR spectrometer (AVATAR 360, Madison, Nicolet). A minimum of 32 scans was signal-averaged with a resolution of 2 cm^{-1} in the 4000–400-cm^{-1} range. UV–vis spectra of WPUA and WPUA/SiO_2 membranes were recorded with a UV–vis spectrometer (UV2450, Shimadzu, Kyoto, Japan) in the 350–800-nm range at 25°C.

Thermal properties

DSC was performed on a Netzsch instrument (204F1, Netzsch, Seligenstadt, Germany). The programmed heating range was from room temperature to 500°C at a heating rate of 10°C/min under a nitrogen atmosphere. The measurement was taken with 6–10 mg samples. DSC curves were recorded.

TABLE II
Some Physical Properties of the WPUA and Hybrid Dispersions

Sample	WPUA	Hyb-1	Hyb-2	Hyb-3	Hyb-4	Hyb-5	Hyb-6
Appearance	#, $	#, $	#, *	#, *	#, *	#, *	#, □
Storage stability (>7 months)	★	★	★	★	★	★	★
Viscosity (Pa·s)	1.346	1.345	1.356	1.342	1.341	1.353	1.348

= microblue; $ = transparent; * = semitransparent; □ = opaque; ★ = no deposit.

SEM

To investigate the morphology of the WPUA and WPUA/SiO_2 membranes, fracture surfaces were investigated with a 20-kV accelerating voltage with a field emission scanning electron microscope (S-4800, Hitachi Corp., Tokyo, Japan).

TEM

The morphology of the composite particles was observed by TEM (TECNAI-12, Philips Co., Eindhoven, Netherlands) with an acceleration voltage of 120 kV. The composite particles were dispersed in deionized water in an ultrasonic bath for 10–30 min and then prepared by the deposition of the emulsion onto a copper net after it was stained by phosphor–wolframic acid.

AFM

AFM topographies were obtained with a Digital Instruments Multimode IIIa atomic force microscope (Veeco Instruments Inc., Plainview, New York, USA) equipped with an E-scanner. Tapping-mode silicon nitride cantilevers TESP with nominal spring constants of 20–100 N/m and nominal resonance frequencies of 200–400 kHz were used. A piece of freshly cleaned mica (ca. 4 × 4 μm^2) was used as a substrate for film preparation. To minimize possible contamination of the surface by ambient air, each sample was freshly prepared just before the AFM experiments.

XRD characterization

The XRD patterns were recorded by the reflection scan with nickel-filtered Cu Kα radiation (D8, Bruker-AXS, Karlsruhe, Germany). The X-ray generator was run at 50 kV and 70 mA. All of the XRD measurements were performed at 2θ values between 3 and 60°.

RESULTS AND DISCUSSION

Properties of the WPUA and WPUA/SiO_2 hybrid material dispersions

The test results of aqueous dispersion, such as storage stability, viscosity, and σ, are shown in Table II. All of the dispersions were stored at room temperature for 7 months and exhibited satisfactory stabilities. The dispersions had little apparent change in viscosity. The storage stability of the WPUA/SiO_2 hybrid dispersions depended on many functions, including pH, solid content, particle size, and viscosity of the medium. Because of the use of DMPA and epoxy–silane (GLYMO) in this study, acting as an internal emulsifier and coupling agent, respectively, the resulting WPUA/SiO_2 hybrid material was also stable.

Compared with the pure WPUA dispersion, the particle sizes of all of the WPUA/SiO_2 hybrid dispersions are shown in Figure 2. Particle size depends on the hydrolysis (rate of nucleation) and condensation rates (rate of growth).[7] The hybrid dispersion had the maximum diameter of 130.1 nm (Hyb-3). With increasing ratio of GLYMO and TEOS, the particle size increased. This was due to the increase in the concentration of epoxy groups and —$Si(OCH_3)_3$; this led to an enhancement in the rates of hydrolysis and the condensation reaction, which consequently, induced the growth of the particles. It was interesting that the curve of particle size showed two cupped peaks, maybe due to the condensation reaction steps of TEOS in WPUA solution following the sequence: nucleation, nucleus propagation forming colloid, and particle growth through

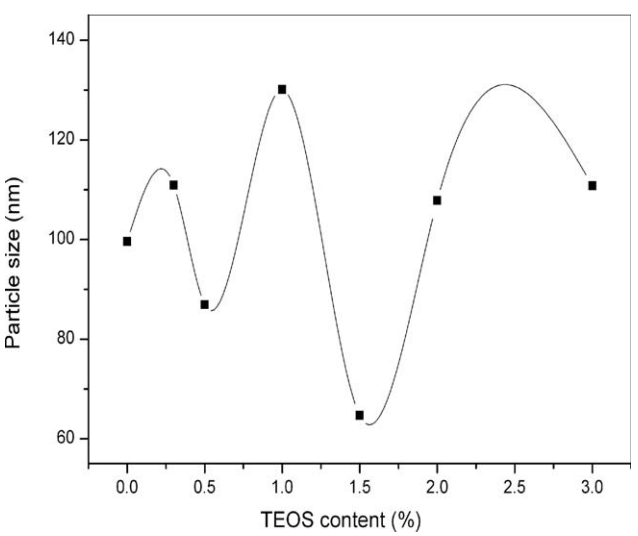

Figure 2 Particle sizes of the WPUA and WPUA/SiO_2 dispersion.

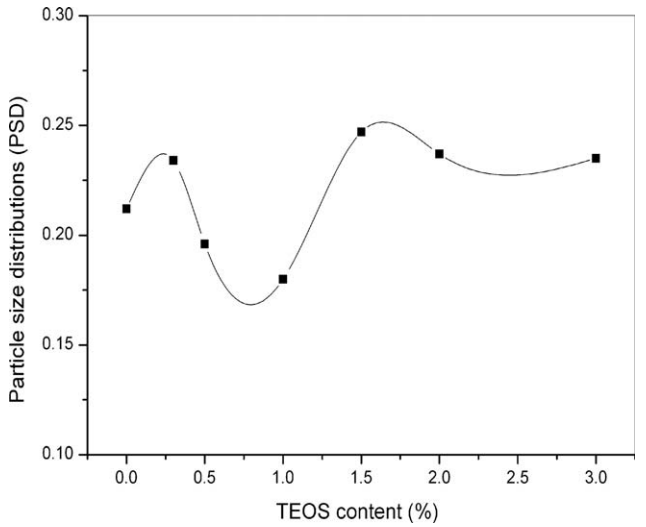

Figure 3 PSDs of the WPUA and WPUA/SiO_2 dispersion.

colloid collision. However, the WPUA chain in solution inhibited particle growth, and the growing particles could not form bigger particles. The PSDs of the WPUA and WPUA/SiO_2 series dispersions are shown in Figure 3. Obviously, the WPUA/SiO_2 hybrids had narrower PSD values than the pure WPUA when the TEOS content was between 0.5–1.0 wt %. The result indicates that there were excellent compatibilities between the organic and inorganic phases.

σ is a phenomenon caused by the cohesive forces between liquid molecules. It is an effect within the surface film of a liquid that causes the film to behave like an elastic sheet. Commonly, it is measured in millinewtons per meter or millijoules per square meter. The knowledge of σ is useful for many applications and processes, as σ governs the chemical and physical behavior of liquids. It can be used to determine the quality of numerous industrial products, such as paints, ink-jet products, detergents, cosmetics, pharmaceuticals, lubricants, pesticides, and food products. Also, it has a profound effect on some steps in industrial processes, such as adsorption, distillation, and extraction. Many methods have been established to measure σ of liquids, such as the capillary rise method, drop weight method, du Nouy ring method, Wilhelmy plate method, spinning drop method, pendant drop method, and sessile drop method. The choice of method depends on the nature and stability of the liquid being measured, measurement conditions, precision, reliability, and instrumentation cost. Among these methods, drop weight can be considered one of the oldest, and it is still widely used. This method is popular because it is inexpensive and the setup is simple. A typical drop weight apparatus consists of a single dripping tip of known diameter, a liquid delivery system, and a weighing balance. In this study, the measurement of σ was conducted on a single-tube manner setup by the maximum air bubble method. The smaller σ is, the better the performance of infiltration is. The σ values of the WPUA and WPUA/SiO_2 hybrid dispersions are listed in Table II. The results show that all of the WPUA/SiO_2 dispersions had smaller σ values than water (72 mN/m). The σ values of all of the hybrids were little bigger than the pure WPUA; this showed an excellent infiltrative performance in the substrate. When the TEOS content reached a certain extent (3.0 wt %), σ increased sharply and showed a relatively poor infiltration performance in substrate.

Mechanical properties of the WPUA and WPUA/SiO_2 hybrids

In the preparation of aqueous dispersions, different substance compositions of the hard segment in the macromolecular chain lead to distinctive molecular weights of prepolymers and, also, variations in the cohesion of PU molecules, which directly impact the mechanical properties of PU membranes.

Figure 4 shows the tensile strength values of the pure WPUA and WPUA/SiO_2 hybrids. From Figure 4, the results indicate that the WPUA/SiO_2 hybrids had higher tensile strengths than the pure WPUA. The curve of tensile strength exhibited a bimodal peak at 0.3 and 1.0 wt %; this showed outstanding mechanical properties. When the TEOS content exceeded 1.0 wt %, the tensile strength value decreased slowly. This was because when the WPUA/SiO_2 hybrids increased in SiO_2 content, the interpenetrating polymer network structure of the WPUA/SiO_2 latex was more compact. The improvement of the mechanical properties could be explained by the results of the formation of the crosslinking.[23,24] The tensile stress of

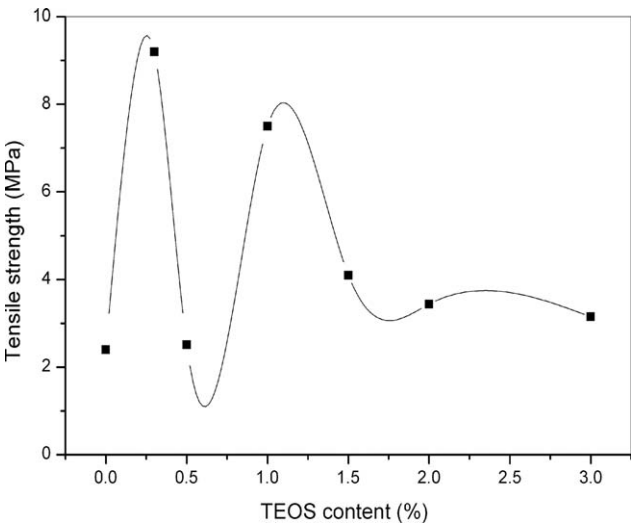

Figure 4 Tensile strength values of the WPUA and WPUA/SiO_2 hybrids.

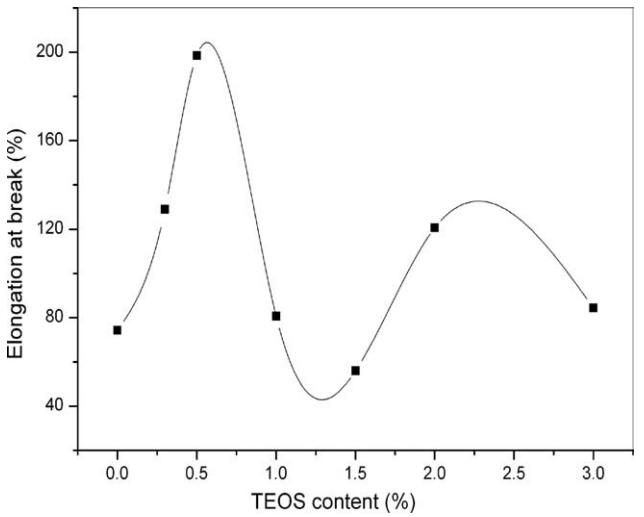

Figure 5 Elongation at break values of the WPUA and WPUA/SiO_2 hybrids.

the hybrid was, of course, dependent on the density of the crosslinking. In other words, the tensile stress should have decreased if there were no bonding sites between the organic polymer phase and the inorganic phase. Moreover, nanosilica (nano-SiO_2), with features of high toughness, large strength, and, also, high physical and chemical reactivity, made it easy for polymer combination to reach the molecular level, which could have been effective in improving the material toughness, ductility, brittleness, and so on. As a result, the mechanical properties of WPU were improved by the modification of the coupling agent and a certain amount of TEOS.

Figure 5 shows the elongation at break values for the pure WPUA and WPUA/SiO_2 hybrids. It was particularly interesting that the elongation at break also increased initially with TEOS content. This was ascribed to the deformation mechanism of WPUA. In the case of WPUA, composed of hard- and soft-segment domains, the hard-segment lamellae, sensitive to applied stress, could be tilted toward the stretching direction at low strain, and in the high strain, they aligned parallel to the stretching direction. Thus, WPUA maintained its stress capacity at a relatively high strain without any breakdown of the amorphous soft chains. Because of the particular flexibility of the macromolecular chain paragraph of the acrylic resin, the hybrid material showed better flexibility, which caused a high elongation at break. In our study, the WPUA/SiO_2 hybrids endured higher stress because of the incorporation of SiO_2, although an excess of SiO_2 negatively affected the elongation of the samples. That is, as the TEOS content increased initially, the formed SiO_2 made the composites more reinforced gradually without hindering elastic deformation of the soft segments; this resulted in higher breaking strengths and elongations at break. However, the incorporation of excess SiO_2 hindered the deformation of soft segments in WPUA and, thus, led to lower elongations at break.

Figure 6 shows the hardness values for the pure WPUA and WPUA/SiO_2 hybrid membranes. The results indicate that the hardness values of the vast majority of hybrid materials were bigger than that of pure WPUA. Because polycondensation was generated by the hydroxyl from the SiO_2 surface and from the hydrolysis of the coupling agent, dimers were first synthesized, and then, gradually we saw a linear, network structure; finally, interpenetrating polymer networks with WPUA were generated, which improved the effect of the interface between the organic and inorganic phases. With increasing SiO_2 content, the structure of the interpenetrating polymer network became more dense; moreover, the microarea formed by the hard segment showed a characteristic large strength, high hardness, and no easy destruction by solvent, so the hardness of the materials increased. However, the hardness of the materials did not increase further with increasing TEOS (SiO_2) content or even decline (e.g., Hyb-6) when the SiO_2 content continued to increase. This is because only when the amount of SiO_2 added to the organic materials was small could the hardness of the membranes improve. Therefore, when the amount of SiO_2 increased to a certain extent, nanoparticles showed a nonuniform dispersed phase, and the hybrids had a decreased toughness.

Figure 7 shows the water absorption for the pure WPUA and WPUA/SiO_2 hybrids. It increased slowly at first, then fell sharply to even lower than that of pure WPUA when the TEOS content was 1.5–3.0%; this enhanced the water resistance. The water absorption reached a minimum of 14.11% when the TEOS

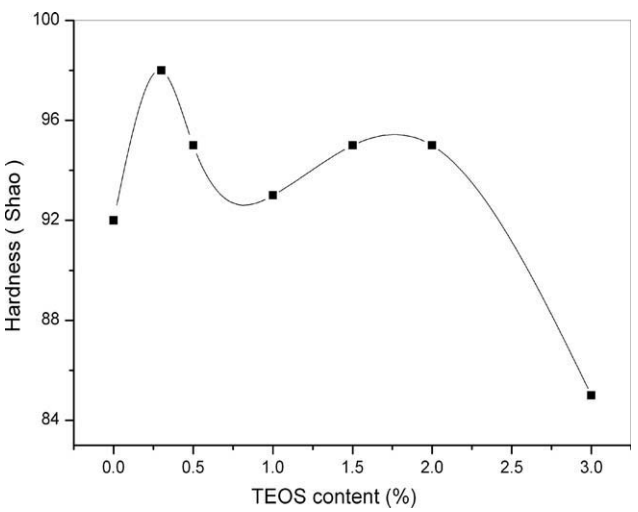

Figure 6 Hardness values of the WPUA and WPUA/SiO_2 hybrids.

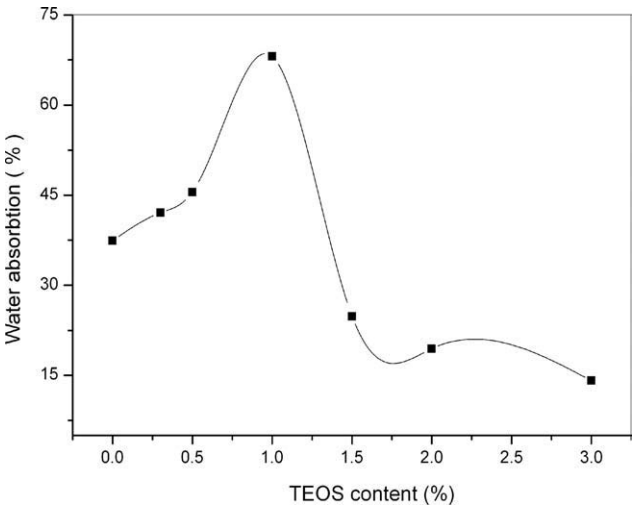

Figure 7 Water absorption values of the WPUA and WPUA/SiO_2 hybrids.

content was 3.0%; this indicated that it had the best water resistance of all of the hybrid materials.

UV–vis spectra of the WPUA and WPUA/SiO_2 hybrids

Transparency is an important parameter for many applications in coatings and films, especially for water-based polymer systems. Figure 8 shows the UV–vis spectra of the WPUA and WPUA/SiO_2 hybrids in the wavelength range 350–800 nm. As shown in the inset (Fig. 8), the transparencies of all of the WPUA/SiO_2 hybrid materials were larger than pure WPUA when the wavelength exceeded 625 nm; this indicated that the hybrid materials possessed excellent transparency in the presence of PA monomers. It also showed that the transmittance at 632 nm decreased from 93% of pure WPUA to 58% of the hybrids with 1.5% TEOS content (Hyb-4) and, then, gradually increased from 58 to 98% for the hybrid with 3.0% TEOS content (Hyb-6). This was because of the smaller refractive index of pure SiO_2 compared to WPUA. Thus, the refractive index decreased with increasing SiO_2 content. At low SiO_2 content, the SiO_2 particle was isolated as a dispersive heterogeneous phase in the hybrid matrix, which resulted in a serious light scattering. This led to a hazy thin film. At high SiO_2 content, the SiO_2 particles were blended into WPUA to form an aggregation phase in the hybrid matrix. This led to an increase in the transparency of the hybrid film. These results suggest that the transparency of the prepared hybrid thin film could be tunable through the adjustment of SiO_2 content.

FTIR spectra of the WPUA and WPUA/SiO_2 hybrids

The IR spectra of the WPUA and WPUA/SiO_2 hybrids are shown in Figure 9. As shown in Figure 9, there was a strong absorption peak at about 1680–1740 cm^{-1}, which corresponded to the carbamate carbonyl of —C=O groups and suggested that more polyester segments and urethane groups interacted with silanol groups on the SiO_2 particles on the basis of the coupling agent. The bands of C—H was observed at 2950 and about 3300 cm^{-1}, respectively. The characteristic absorption of the C=C bond at 1640 cm^{-1} disappeared; this indicated that the acrylic monomers were polymerized. In all of the spectra, the strong peak around 3350 cm^{-1} came from the stretching vibration of N—H bonds in the urethane segments. As the peak at 1538 cm^{-1} belonged to N—H groups, the height of the N—H peak decreased

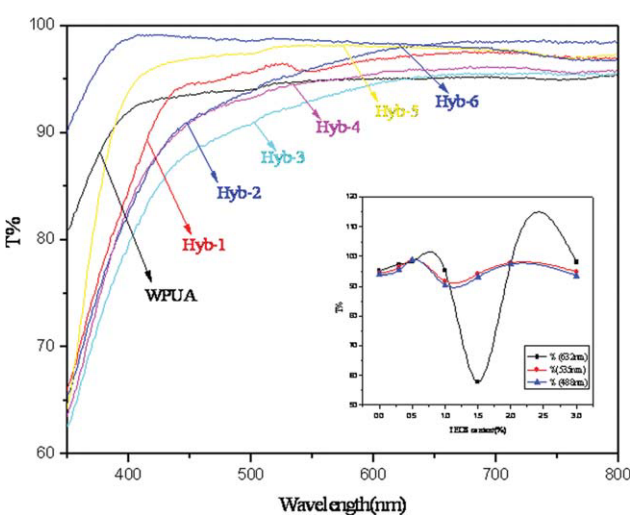

Figure 8 UV–vis spectra of the WPUA and WPUA/SiO_2 hybrids. [Color figure can be viewed in the online issue, which is available at wileyonlinelibrary.com.]

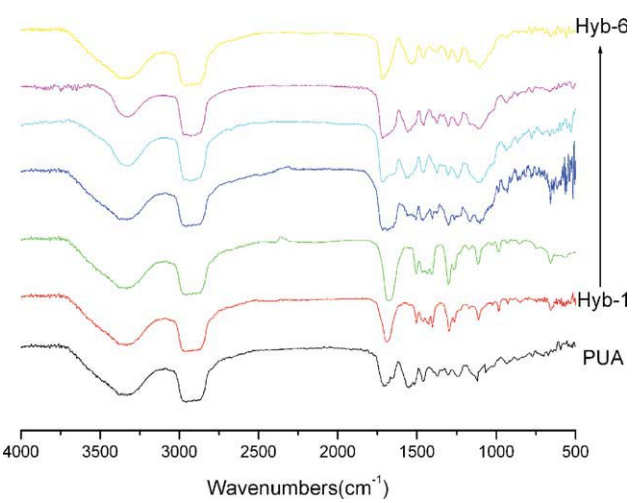

Figure 9 FTIR spectra of the WPUA and WPUA/SiO_2 hybrids. [Color figure can be viewed in the online issue, which is available at wileyonlinelibrary.com.]

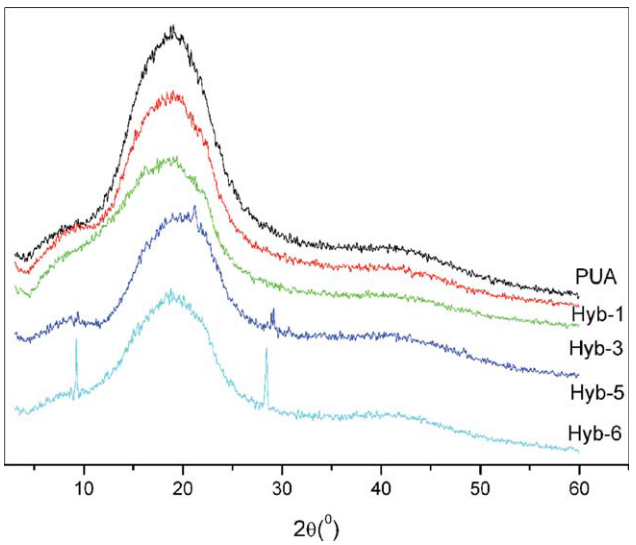

Figure 10 XRD curves of the WPUA and some WPUA/SiO_2 hybrids. [Color figure can be viewed in the online issue, which is available at wileyonlinelibrary.com.]

after radical polymerization, which indicated the interactions of N—H groups with the acrylate component. Clearly, there were wide and strong absorption peaks from 1050 to 1150 cm^{-1} in the samples of all of the hybrid materials, which showed the existence of a Si—O—Si backbone, which was due to the polycondensation between the siloxane side the of coupling agent GLYMO and the hydrolysis of TEOS, which formed an Si—O—Si network and generated an interpenetrating polymer network between the organic and inorganic phases. The absorption peak was broader with increasing SiO_2 content. Also, there was a weak absorption peak at about 930 cm^{-1}, which corresponded to the Si—O—C bond in the samples of the hybrid materials; this indicted that it was not a simple mixture of silicon dioxide and PU but the bonding of some kind of chemical bond. Therefore, it formed a strong bond-linked complex hybrid interaction system between the organic polymer and the inorganic phase, which weakened the key single-phase body and provided the basis for the excellent performance of the hybrid materials.

XRD of the WPUA and WPUA/SiO_2 hybrids

XRD is the most powerful technique for monitoring the formation and structure of intercalated layers. Figure 10 shows the XRD curves for WPUA and some WPUA/SiO_2 hybrids. For pure WPUA, a nearly amorphous diffraction peak was seen near $2\theta = 20°$;[21] this indicated the crystallinity of polyester segments. In addition, a diffused diffraction peak appeared near 20° for all of the WPUA/SiO_2 nanocomposites, and this peak was attributed to the short-range-order arrangement of chain segments of amorphous PU and the formation of a uniform three-dimensional network structure, which was interspersed with the WPUA segment. In the hybrid patterns, the XRD diffractions of Hyb-1 and Hyb-3 were similar, and there were no other diffraction peaks, which indicated that SiO_2 in the WPU matrix was exfoliated or intercalated. Organic and inorganic uniform cross networks were formed between SiO_2 and WPUA, which limited SiO_2 nucleation and crystal growth. However, two diffraction peaks emerged at about $2\theta = 9.0$ and 28.5°(Hyb-5 and Hyb-6), and their intensities increased with increasing SiO_2 content. These diffraction peaks corresponded to the secondary diffraction peaks of SiO_2.

SEM of the WPUA and WPUA/SiO_2 hybrids

The cross sections of WPUA and Hyb-1 observed by SEM are shown in Figure 11. Evidently, the surface of WPUA/SiO_2 was relatively smooth and with almost no cracks, comparatively; it showed some relatively rule cracks in the hybrid materials, and the majority of white spots emerged at the bottom of the cracks, which indicated that the existence of SiO_2 particles was the cause of cracks. The existence of cracks showed that the fracture region extended along the SiO_2 particles so

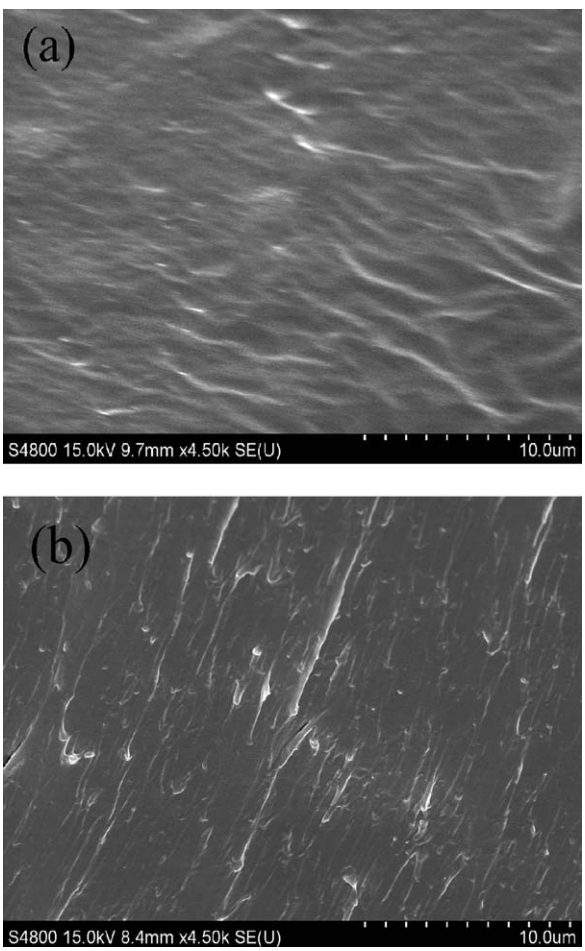

Figure 11 SEM photographs of (a) WPUA and (b) Hyb-1.

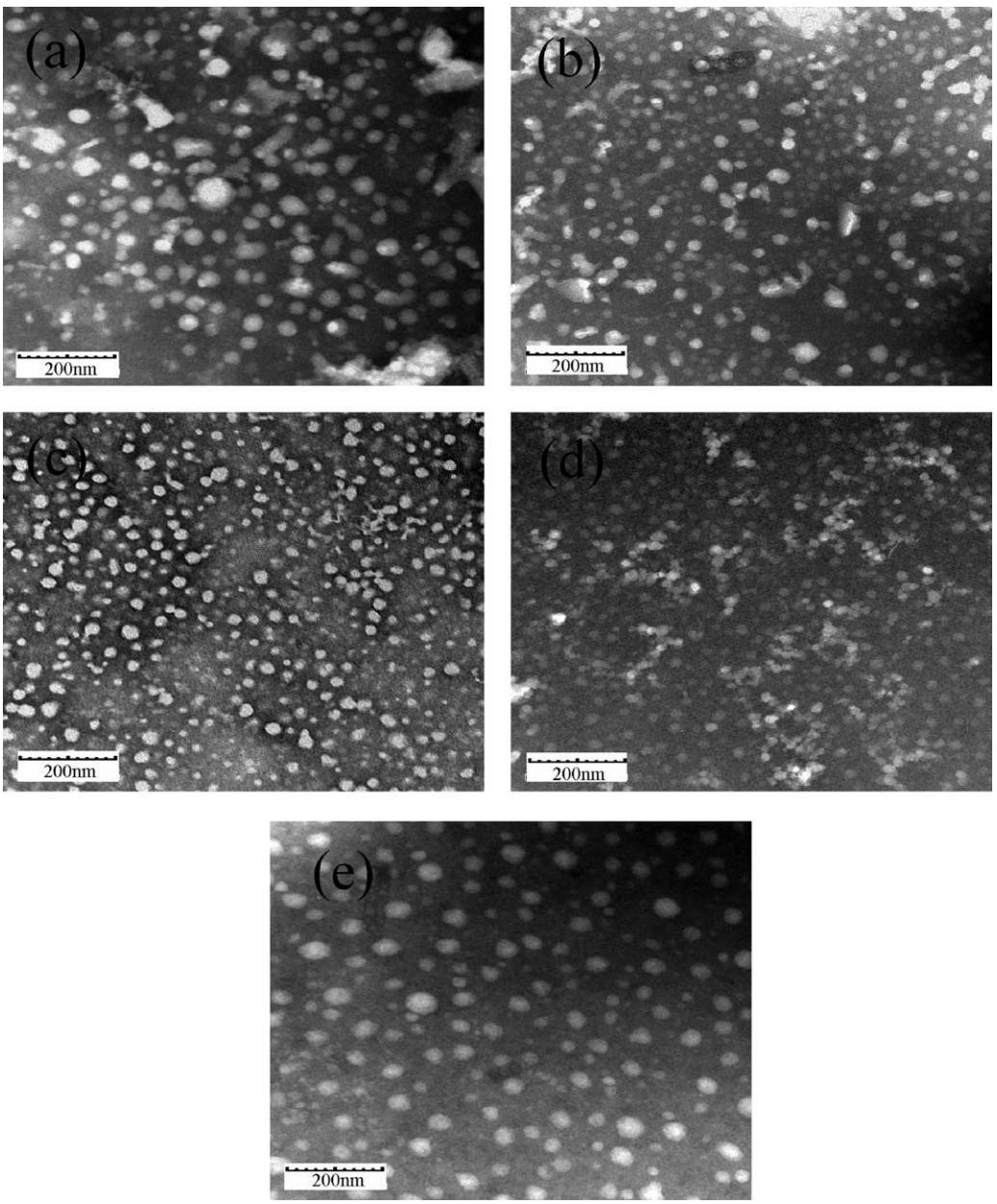

Figure 12 TEM photographs of (a) WPUA, (b) Hyb-1, (c) Hyb-3, (d) Hyb-5, and (e) Hyb-6.

that SiO_2 particles dispersed in the body of WPUA/SiO_2. The rule cracks indicated that the particles were uniformly dispersed in the WPUA/SiO_2 system, which weakened the agglomeration phenomena. The inorganic SiO_2 particles were embedded in the organic–inorganic network structure; in other words, a three-dimensional inorganic network was introduced into the system, and inorganic particles were besieged by the organic phase, which acted as the continuous phase.

TEM of the WPUA and WPUA/SiO_2 hybrids

To obtaining further characterization of membranes, such as the microphase structure and compatibility, TEM micrographs of the WPUA and WPUA/SiO_2 hybrids were observed and are shown in Figure 12. As shown in Figure 9, we could clearly identify a considerable number of nanoscaled SiO_2 particles dispersed uniformly in the WPUA matrix; this was mainly because nano-SiO_2 was effectively limited to the regular molecular network structure of PUA. On the other hand, covalent bonding (Si—O—Si) between the organic and inorganic components enhanced the miscibility. They were homogeneously and uniformly dispersed at a molecular level. The formation SiO_2 particles in the as-prepared WPUA and coupling agent GLYMO matrix indicated that the —$Si(OCH_3)_3$ groups may have functioned as internal bridging groups between the organic and

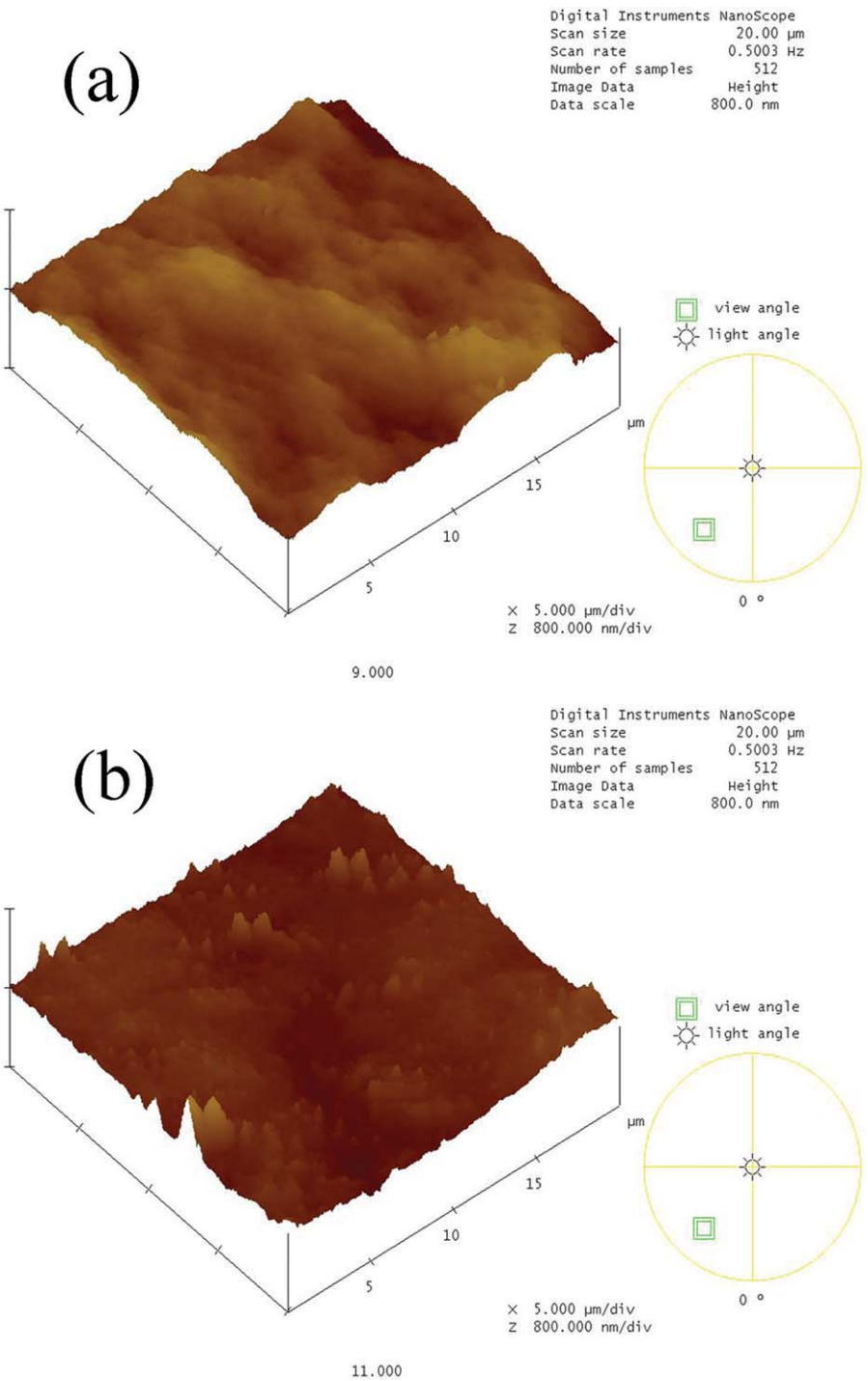

Figure 13 AFM photographs of (a) WPUA and (b) Hyb-3. [Color figure can be viewed in the online issue, which is available at wileyonlinelibrary.com.]

inorganic segments for sol–gel reactions of the TEOS molecules. The condensation reaction steps of TEOS in the WPUA solution were in the following sequence: nucleation, nucleus propagation forming colloid, and particle growth through colloid collision. However, the WPUA chain in solution inhibited the particle growth. Therefore, the particle size was about 10–40 nm, as shown in Figure 12, and the size slightly increased as the SiO_2 content increased. The increase in the SiO_2 particle size clearly resulted from the increase in the aggregation tendency as the TEOS content and the SiO_2 particle number increased. These micrographs show the fine interconnected or cocontinuous phases morphologies. We estimate that these materials will be pretty good for practical applications.

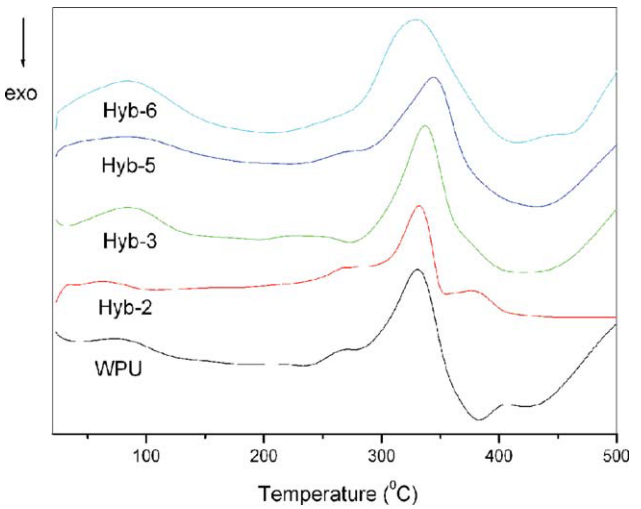

Figure 14 DSC curves of WPUA and the hybrids. [Color figure can be viewed in the online issue, which is available at wileyonlinelibrary.com.]

AFM of the WPUA and WPUA/SiO_2 hybrids

AFM study demonstrated an accurate photopattern of the hybrid film surface. Figure 13 shows three-dimensional AFM images of WPUA and Hyb-3. The hybrid showed a rough surface morphology, whereas the pure WPUA film had a much smoother appearance. This was because the lower surface energy of the TEOS molecule with hydrophobic groups created surface roughness, which resulted in an increase in the surface area. Such a surface morphology enhanced the water resistance and the friction resistance. A number of small bulges were observed on the interfaces, as shown in Figure 13. The bulges should have been SiO_2 particles because the size of the bulges varied with the particle size of SiO_2 and so was close to the particle size of the SiO_2 used; this indicated that some nano-SiO_2 particles existed at the interfaces.

Thermal properties of the WPUA and WPUA/SiO_2 hybrids

Figure 14 shows the DSC scan curves for the WPUA and WPUA/SiO_2 hybrids. The WPUA/SiO_2 membranes had a higher glass-transition temperature of hard segments than the WPUA membrane. There was only one glass-transition temperature in the all of the membrane samples. The result indicates that polymers were almost completely compatible; this phenomenon existed because of the copolymerization between the organic polymer WPUA and inorganic components, which greatly improved the compatibility, close to the mixed molecular level.

CONCLUSIONS

A series of WPUA/SiO_2 membranes were synthesized by a sol–gel process. The WPUA/SiO_2 compounds showed a homogeneous morphology, which supported the compatibility improvements shown by SEM, TEM, and AFM measurements. Compared with a WPUA aqueous dispersion, the particle sizes of the hybrid aqueous dispersion increased from 64.7 to 110.9 nm. The thermal and mechanical properties of the WPUA/SiO_2 composite membranes were much better than those of pure WPUA; this was due to chemical network formations between the organic and inorganic phases. The optical transparency did not linearly decrease with increasing SiO_2 fraction in the hybrid thin film but increased with the TEOS content in the presence of acrylate monomers. The results also show that the prepared membranes demonstrated a tunable transparency with the SiO_2 fraction in the membranes.

References

1. Bai, C. Y.; Zhang, X. Y.; Dai, J. B.; Li, W. H. Prog Org Coat 2006, 55, 291.
2. Bai, C. Y.; Zhang, X. Y.; Dai, J. B. Prog Org Coat 2007, 60, 63.
3. Deng, X.; Liu, F.; Luo, Y.; Chen, Y.; Jia, D. Prog Org Coat 2007, 60, 11.
4. Deng, X.; Liu, F.; Luo, Y.; Chen, Y.; Jia, D. Eur Polym J 2007, 43, 704.
5. Zhou, X.; Tu, W.; Hu, J. Chin J Chem Eng 2006, 14, 99.
6. Zhang, C.; Zhang, X.; Dai, J.; Bai, C. Prog Org Coat 2008, 63, 238.
7. Hu, G.; Shen, H.; Fu, H.; Chen, H. J Wuhan Univ Technol 2008, 23, 41.
8. Kim, E. H.; Myoung, S. W.; Jung, Y. G.; Paik, U. Prog Org Coat 2009, 64, 205.
9. Okamoto, Y.; Hasegawa, Y.; Yoshino, F. Prog Org Coat 1996, 29, 175.
10. Li, Y. K.; Ling, A. L.; Sang, H. X.; Wu, Q. New Chem Mater (in Chinese) 2000, 28, 31.
11. Zhou, S. K.; Lin, J. Q.; Xu, Y. T.; Dai, L. Zhanjie (in Chinese) 2001, 22, 21.
12. Xie, X. L.; Li, R. K.; Liu, Q. X.; Mai, Y. W. Polymer 2004, 45, 2793.
13. Rupali, G.; Amitabha, D. Chem Mater 2000, 12, 608.
14. Vollath, D.; Szabo, D. V.; Schlabach, S. J Nanopart Res 2004, 6, 181.
15. Yeh, J. M.; Yao, C. T.; Hsieh, C. F. Eur Polym J 2008, 44, 2777.
16. Kim, D. S.; Park, H. B.; Rhim, W.; Lee., Y. M. J Membr Sci 2004, 240, 37.
17. Kulkarni, S. S.; Tambe, S. M.; Kittur, A. A.; Kariduraganavar, M. Y. J Membr Sci 2006, 285, 420.
18. Suryani; Liu, Y. L. J Membr Sci 2009, 332, 121.
19. Chattopadhyay, D. K.; Muehlberg, A. J.; Webster, D. C. Prog Org Coat 2008, 63, 405.
20. Chattopadhyay, D. K.; Zakula, A. D.; Webster, D. C. Prog Org Coat 2009, 64, 128.
21. Bonilla, G.; Martínez, M.; Mendoza, A. M.; Widmaier, J. M. Eur Polym J 2006, 42, 2977.
22. Guo, Z.; Kim, T. Y.; Lei, K.; Pereira, T.; Sugar, J. G.; Hahn, H. T. Compos Sci Technol 2008, 68, 164.
23. Zhu, Z. K.; Yang, Y.; Yin, J.; Qi, Z. N. J Appl Polym Sci 1999, 73, 2977.
24. Wang, L. W.; Ye, T.; Ding, H. Y.; Li, J. D. Eur Polym J 2006, 42, 2921.